RESEARCH ARTICLE

Check for updates

physica
status
solidi
pssrrl

www.pss-rapid.com

Effect of Cap Thickness on InAs/InP Quantum Dots Grown by Droplet Epitaxy in Metal–Organic Vapor Phase Epitaxy

Elisa M. Sala,* Max Godsland, Aristotelis Trapalis, and Jon Heffernan

InAs quantum dots (QDs) are grown on bare InP(001) via droplet epitaxy (DE) in metal–organic vapor phase epitaxy (MOVPE). Capping layer engineering, used to control QD size and shape, is explored for DE QDs in MOVPE. The method allows for the tuning of the QD emission over a broad range of wavelengths, ranging from the O- to the L-band. The effect of varying the InP capping layer is investigated optically by macro- and micro-photoluminescence (PL, µPL) and morphologically by transmission electron microscopy (TEM). A strong 500 nm blueshift of the QD emission wavelength is observed when the capping layer is reduced from 20 to 8 nm, which is reflected by a clear size reduction of the buried QDs.

1. Introduction

Owing to their appealing physical properties, semiconductor quantum dots (QDs) have attracted great attention for a broad range of applications, ranging across lasers and amplifiers,[1–3] nanomemories,[4–6] and recently as efficient sources of single and entangled photons for quantum information technologies.[7–10] III–V QDs fabricated by droplet epitaxy (DE) have shown a great degree of flexibility in terms of variety of nanostructures possible and material choice,[11–14] resulting in improved compositional homogeneity and symmetry, and reduced strain.[11,15,16] Also, the method allows for increased control of the associated wetting layers in QD growth.[17–19] Such properties are particularly appealing for their application as building blocks for quantum

Dr. E. M. Sala, Dr. A. Trapalis, Prof. J. Heffernan
EPSRC National Epitaxy Facility
The University of Sheffield
North Campus, Broad Lane, Sheffield S3 7HQ, UK
E-mail: e.m.sala@sheffield.ac.uk

Dr. E. M. Sala, M. Godsland, Dr. A. Trapalis, Prof. J. Heffernan
Department of Electronic and Electrical Engineering
The University of Sheffield
North Campus, Broad Lane, Sheffield S3 7HQ, UK

The ORCID identification number(s) for the author(s) of this article can be found under https://doi.org/10.1002/pssr.202100283.

information platforms where exceptionally high quality QDs are required. DE has been extensively explored by molecular beam epitaxy (MBE)[11–14] It is only more recently that it has been successfully applied to MOVPE, where promising results have been obtained: for instance, InAs/InP QDs grown via DE in MOVPE have been used in the first entangled quantum light-emitting diode (QLED) emitting in the telecom C-band[15] and in qubit teleportation.[17,19] Our recent study of growth conditions for DE of InAs/InP QDs demonstrated the ability to form QDs in local etched pits,[18] creating the possibility to engineer through the epitaxy process more complex and novel nanostructures.

Here, we apply an epitaxial engineering technique to InAs/InP DE QDs, namely, the variation of the InP capping layer thickness deposited above the QDs, to obtain broad emission wavelength tuning. This is an important element in the scale-up and exploitation of QD-based photonic devices. Epitaxially grown III–V QDs are commonly overgrown by a thin capping layer, typically of the same material as the substrate and usually at the same QD growth temperature, to bury the QDs before further growth. This epitaxial technique can be used to induce shape modifications in the dots and control the emission wavelength.[20–27] Occasionally, also different materials are explored for strain engineering and/or to intentionally alter the QD composition.[28–32] This technique has been used for QDs grown via Stranski–Krastanov (SK) in MOVPE[28,29,31,32] and MBE[20–24] or, less commonly, by DE in MBE.[33] In this work, we demonstrate the possibility to use capping layer engineering for DE QDs grown by MOVPE. To study the effect of the capping layer thickness, buried QDs have been grown with a low-temperature InP layer cap whose thickness varies from 8 to 20 nm and is deposited just after the QD crystallization step. The QDs have been characterized morphologically with transmission electron microscopy (TEM), and optically with room-temperature photoluminescence (RT–PL) and low-temperature micro-PL (LT–µPL).

2. Sample Fabrication

All samples were grown in a close-coupled showerhead (CCS) MOVPE reactor, using H_2 as carrier gas. Indium droplets were first deposited on an InP buffer layer of thickness 300 nm which grown at 600 °C. The droplets were deposited at 320 °C and

ADVANCED SCIENCE NEWS
www.advancedsciencenews.com

pss rrl
physica status solidi
www.pss-rapid.com

thereafter crystallized into InAs QDs under an AsH₃ flow whilst ramping the temperature to 520 °C. The choice of this specific crystallization temperature proved to be the optimum for obtaining high-quality QDs in our growth experiments.[18] We note that these growth parameters yield a QD density of $\approx 9 \times 10^{8}$ cm^{-2}.[18] After complete crystallization, an InP capping layer with variable thickness was grown at the same temperature of 520 °C and the structures were completed with an 80 nm InP layer grown at 600 °C. For additional details on the growth sequence, we refer to our previous work.[18]

3. Results and Discussion

A first insight into the effect of the capping layer on the buried QDs is found through TEM analysis. **Figure 1,2** show TEM images of buried InAs/InP QDs corresponding to QD samples with varying capping thickness in the range of 8–20 nm. TEM images are taken under (002) dark-field diffraction conditions allowing layers structure and compositional information to be distinguished by dark/bright contrast. Such imaging conditions are sensitive not only to compositional variations but also partially to strain fields.[34] Here, regions showing darker contrast correspond to As-containing material, and contrast well with the lighter InP background. Overall, no defects or dislocations can be found, revealing the high quality of the grown material. Figure 1 a,b shows QDs with 20 and 15 nm capping layers, respectively.

The images show the presence of QDs having truncated-pyramidal shapes, as is typically observed for buried QDs.[22,25,35] In fact, during the capping procedure, III–V In-based QDs normally undergo shape modification and material redistribution[20,22,25] with the original QD height decreasing during the cap material deposition as indium outdiffuses toward the QD's lateral flanks.[22,25] This process results in the formation of the typical truncated-pyramid shape.[22,25,35] A thick capping layer generally ensures this process is fully developed and results in formation of large QDs. In Figure 1,2, we also observe "halos," i.e., bright and dark diffused regions around each QD, especially for the thicker capping layers of 20 and 15 nm. These are ascribed
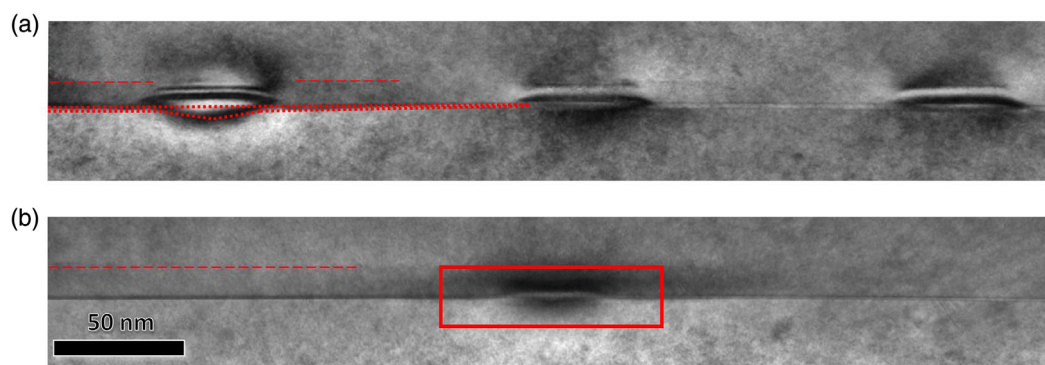

Figure 1. a,b) TEM images of buried InAs/InP QDs having variable capping layer thicknesses of 20 nm (a) and 15 nm (b), taken under dark field (002) diffraction conditions.
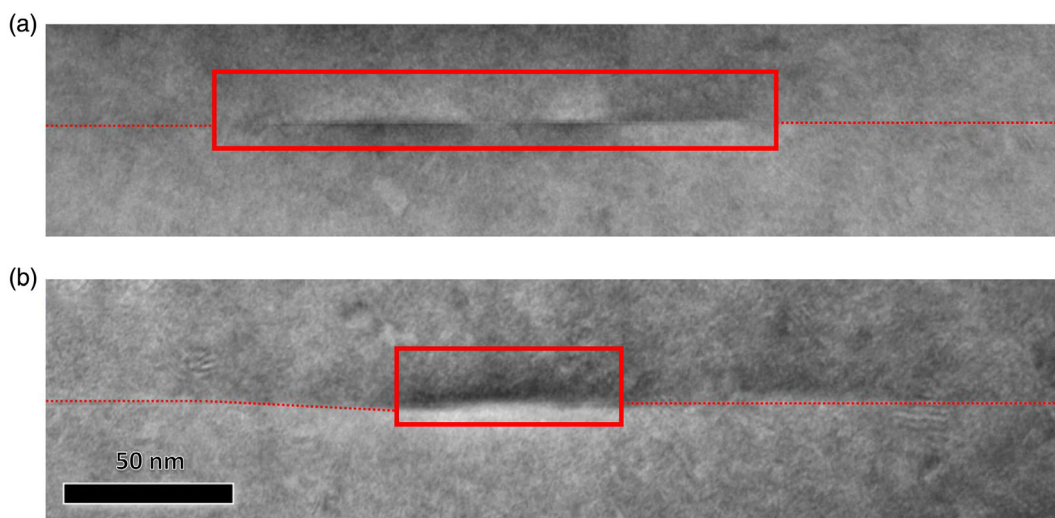

Figure 2. a,b) TEM images of buried InAs/InP QDs having variable capping layer thicknesses of 10 nm (a) and 8 nm (b), taken under dark field (002) diffraction conditions.

to variations of the strain field close to the QDs. In fact, the (002) family planes around the QDs bend due to strain effects, while additional dynamical effects involving the more strain-sensitive (004) diffracted beams take place.[34] As a result, halos become visible, being more pronounced for thicker parts of the specimen.[34] Nevertheless, this phenomenon does not affect our ability to estimate the size of the QDs at first order. For all investigated samples, there is a 2D nonstoichiometric $InAs_xP_{1-x}$ quasi-wetting layer, which is formed in-between the QDs[15,16,18] due to exposure of the InP interdot surface during the crystallization phase.[18] This is also visible as a straight line in-between the QDs in TEM. However, we note in Figure 1a that this layer appears to bend close to the QD on the left-hand side, illustrated by the red dotted lines as a guide for the eye. We see the same effect around a QD with a thinner cap of 8 nm in the left-hand side of Figure 2b which we ascribe to the dot sitting in an etched pit. Although difficult to precisely address such features with TEM, we can reasonably infer that this effect corresponds to the local etching of the 2D layer around the QDs discussed in our previous work.[18] The reduction of the capping layer grown above the QDs has a strong impact on their size. The QDs visibly shrink with thin capping layers, especially for 10 and 8 nm, as shown in Figure 2a,b. Here, the QDs (highlighted with red squares) appear as much flatter objects compared with those shown in Figure 1a,b. Also, the diffused "halo" regions around them are suppressed. This points to a decreased strain field, which is consistent with the reduced size of the QD for thinner caps. **Figure 3**a shows the trend of the QD heights and widths against the capping layer thickness, from the analysis of a number of QDs.

Compared with surface QDs measured by atomic force microscopy (AFM),[18] which showed free-standing heights of ≈10–15 nm, the buried QD heights are overall strongly reduced. We also observe QD widths to be dependent on capping thickness starting with a width of ≈60 nm for 20 nm capping layer and reducing to ≈40 nm for an 8 nm cap. Therefore, we directly

observe that the capping process strongly modifies the shape and size of the QDs. We propose a mechanism for the capping process, as shown in Figure 3b–d. The capping process begins with the supply of InP at a low temperature of 520 °C.[18] Indium outdiffuses from the QD apex and flows toward the QD flanks, as shown in Figure 3b, similar to what is observed for other III–V QD systems, for instance, InAs/GaAs QDs.[22] Thereby the dissolution of the QD has started, and its height gradually reduces while the capping layer is growing and both In and As are released. In Figure 3b, we include the presence of arsenic with yellow circles and assume the surface is As-terminated because we know that the 2D layer of InAsP is formed during the preceding crystallization process.[18] Next, the released In accumulates at the QD base and contributes to its width increase by bonding with the arsenic available on the surface (see **Figure 3**c). Once the capping layer deposition has completed, the InP supply ceases, and the temperature is ramped up to 620 °C in preparation for the growth of the high-temperature InP burying layer that completes the structure and provides for good optical properties in surrounding layers.[18] During this high-temperature growth, phosphorous is continuously supplied for surface stabilization. The phosphorous supply together with the rise in temperature can easily destroy the remaining uncapped parts of the QD protruding through the capping layer by enhancing the As–P exchange[26] and thermally inducing In desorption. Here, it is important to point out that the heights of the final capped QDs are significantly smaller than the nominal thickness of the deposited InP as capping material. For instance, for 20 nm nominal capping the resulting QDs are ≈5 nm high, as shown in Figure 3a, and their heights decrease further with the nominal cap thickness reduction. We believe the actual thickness of the capping layers is smaller than the nominal thickness. The growth rate for the low-temperature capping layers was calibrated using thick layers and not on QD/2D surface. When thin caps are grown on a surface containing significant amounts of excess
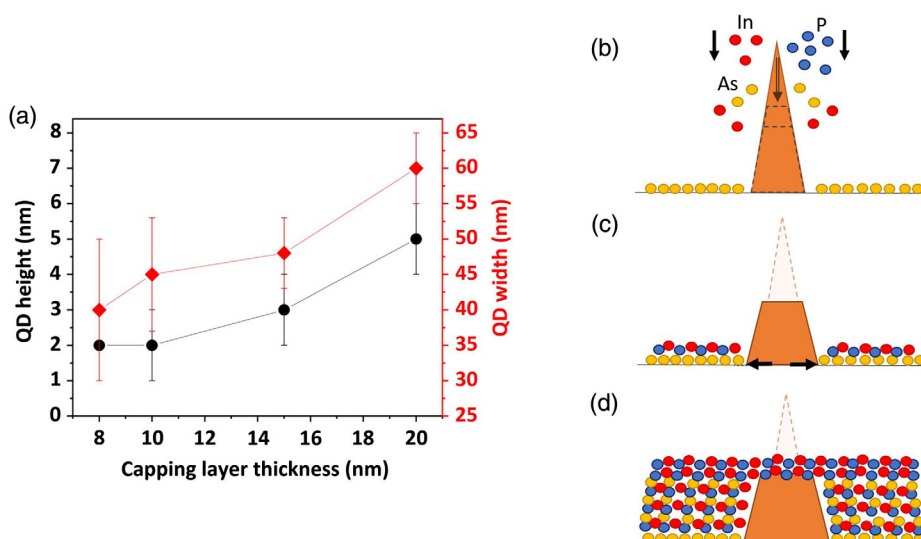

Figure 3. a) Plot of QD height and width versus capping thickness. b–d) Sketch of the capping process for a single QD capped with InP. The QD is represented by the orange (truncated) pyramid. The circles represent In and P supplied as capping material, in red and blue, respectively. The yellow circles represent As released during the QD demolition and the excess As present on the surface.
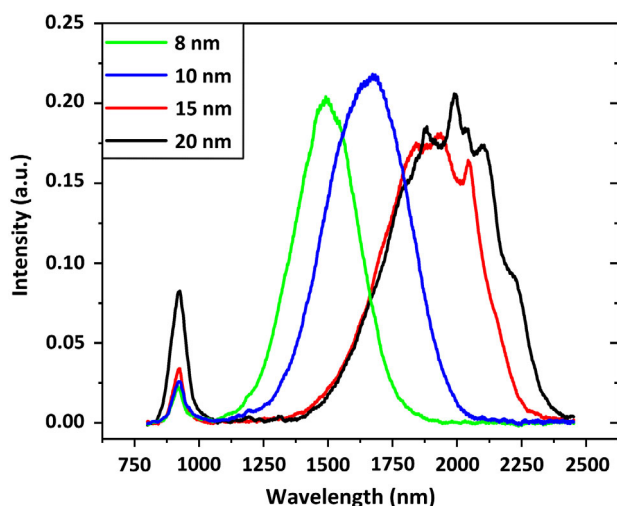
Figure 4. PL spectra at room temperature of QD ensembles with varying cap thickness ranging from 8 to 20 nm.

arsenic on the 2D InAsP layer, we believe the growth rate to be reduced. This would then explain why even in the case of a nominally 20 nm capping layer the dots are only 5 nm high after the capping process, something we would not expect if the cap was indeed 20 nm thick because no part of the QD would protrude above the cap during the high-temperature growth. This conjecture is supported by evidence in Figure 1a,b which shows a slightly darker contrast in the first 10–12 nm of the InP above the dots (shown by the dotted red line) (also sketched in Figure 3d). We believe this is due to the incorporation of surface As into the InP cap during growth. We expect this only occurs during the cap growth and hence suggests the real thickness of InP is around half the nominal thickness and possibly less.

Figure 4 shows RT–PL spectra of the QDs. The measurements were conducted by using a 645 nm diode laser with 75 W cm^{-2} power density. The emission around 920 nm, detected for all samples, is ascribed to the InP substrate,[36] while the broader peak at longer wavelengths is identified as the QD emission.[18] Varying the cap thickness between samples, in the nominal range 8–20 nm, leads to a dramatic redshift of the ensemble dot emission by approximately 500 nm, covering wavelengths from 1200 to 2400 nm. The observed redshift in PL is consistent with the increase in QD size seen in TEM and the effects of quantum confinement.[20–24,37]

Next, the same QD samples have been investigated via μPL at 4 K. For μPL, the samples were excited using a fiber-coupled 635 nm diode laser at power densities of approximately 2.24 and 717 W cm^{-2} at low- and high-power measurements, respectively. The PL was collected using a 100× objective (Mitutoyo M Plan Apo NIR 100X, numerical aperture [NA]=0.5) and the collection area was approximately 5 μm in diameter. The corresponding spectra are shown in **Figure 5**a,b.

Figure 5a shows that emission from single QDs is detected in a range of ≈500 nm as observed in macro-PL measurements at room temperature, although the spectra are considerably more complicated than the ensemble macro-PL. Capping the QDs with layers as thick as 20 nm results in single-dot emission at 4 K at the telecom C-band and up to the 1600 nm detector cutoff. The general trend previously observed in RT–PL can be found also for single-dot emission, where QDs capped with 8 and 10 nm mostly emit at short wavelengths up to ≈1400 nm (spectral regions marked with "A" and "B" in Figure 5a. However, in high-excitation μPL shown in Figure 5b, we observe the presence of a long-wavelength emission emerging as the cap thickness is increased from 10 nm caps upward. We attribute this to the emergence of electronic states in the C-band, belonging to small QDs not fully formed when thin capping layers are used and thus not yet
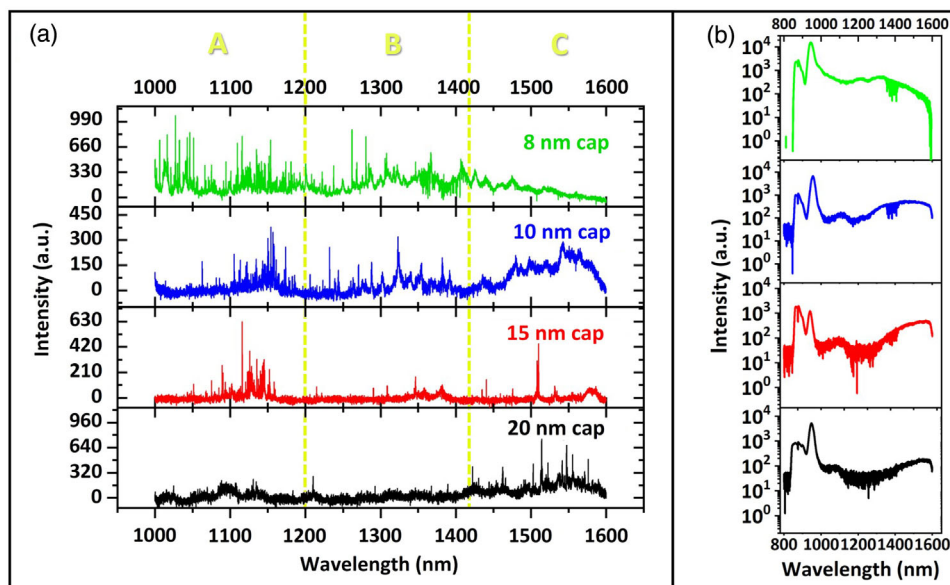

Figure 5. a) Low-excitation μPL measurements conducted at 4 K of the QD samples having cap thickness of 8–20 nm. Indication of the cap thickness is provided in each frame. b) Corresponding high-excitation μPL (log scale). Same color scale as in Figure 4.

detectable as efficient single-dot lines in the low-excitation μPL. The dense single lines detected in regions A and B, for thin caps we ascribe to two phenomena: 1) emission from small QDs and 2) exciton trapping at monolayer (ML) fluctuations of the 2D non-stoichiometric $InAs_xP_{1-x}$ quasi-wetting layer, formed during the QD crystallization phase.[18,38,39] This is most evident in the strong emission seen around 900–1100 nm in the high-excitation region in Figure 5b. We note that many of the short wavelength single lines of region A are quenched with thicker caps and for 15 and 20 nm caps, the QD lines in region B are also quenched and the emissions in region C starts to dominate. At 20 nm, the short-wavelength PL in A and B is almost completely quenched and single-dot lines are observed mostly at long wavelengths up to 1600 nm. As it is not expected that the thicker caps effect the 2D InAsP layer, this behavior suggests a preferential carrier capture and recombination into larger QDs.[37] Overall, the RT–PL and μPL investigations presented here find good agreement with the TEM analysis discussed earlier, where we found that reducing the thickness of the low-temperature capping layers grown above the QDs leads to a size reduction of the buried QDs.

4. Conclusions

We applied a capping layer engineering method to InAs/InP QDs grown by droplet epitaxy in MOVPE. Morphological investigations of buried QDs via TEM showed a strong dependence of QD size on capping layer thickness which led to a tuning of the QD emission wavelength over 500 nm, including the O- and L- and C-bands. We demonstrated for the first time the possibility to use the capping layer engineering for InAs/InP QDs fabricated by droplet epitaxy in MOVPE, which can be used as an on-demand tuning of the emission wavelength of such QDs over a broad range of technologically relevant wavelengths.

Conflict of Interest

The authors declare no conflict of interest.

Data Availability Statement

The data that support the findings of this study are openly available in The University of Sheffield's data repository, ORDA, at https://doi.org/10.15131/shef.data.14680086.

[1] D. Bimberg, N. Kirstaedter, N. N. Ledentsov, Z. I. Alferov, P. S. Kopev, V. M. Ustinov, *IEEE J. Sel. Top. Quantum Electron.* **1997**, *3*, 196.

[2] H. Schmeckebier, D. Bimberg, *Green Photonics And Electronics*, Springer, Cham, Switzerland **2017**.

[3] F. Heinrichsdorff, M. H. Mao, N. Kirstaedter, A. Krost, D. Bimberg, A. O. Kosogov, P. Werner, *Appl. Phys. Lett.* **1997**, *71*, 22.

[4] A. Marent, T. Nowozin, M. Geller, D. Bimberg, *Semicond. Sci. Technol.* **2011**, *26*, 014026.

[5] L. Bonato, I. F. Arikan, L. Desplanque, C. Coinon, X. Wallart, Y. Wang, P. Ruterana, D. Bimberg, *Phys. Status Solidi B* **2016**, *5*, 1877.

[6] E. M. Sala, I. F. Arikan, L. Bonato, F. Bertram, P. Veit, J. Christen, A. Strittmatter, D. Bimberg, *Phys. Status Solidi B* **2018**, *255*, 1800182.

[7] S. Hepp, M. Jetter, S. L. Portalupi, P. Michler, *Adv. Quantum Technol.* **2019**, *2*, 1900020.

[8] C. L. Salter, R. M. Stevenson, I. Farrer, C. A. Nicoll, D. A. Ritchie, A. J. Shields, *Nature* **2010**, *465*, 594.

[9] A. Schlehahn, M. Gaafar, M. Vaupel, M. Gschrey, P. Schnauber, J.-H. Schulze, S. Rodt, A. Strittmatter, W. Stolz, A. Rahimi-Iman, T. Heindel, M. Koch, S. Reitzenstein, *Appl. Phys. Lett.* **2015**, *107*, 041105.

[10] T. Müller, J. Skiba-Szymanska, A. B. Krysa, J. Huwer, M. Felle, M. Anderson, R. M. Stevenson, J. Heffernan, D. A. Ritchie, A. J. Shields, *Nat. Commun.* **2018**, *9*, 862.

[11] M. Gurioli, Z. Wang, A. Rastelli, T. Kuroda, S. Sanguinetti, *Nature Materials* **2019**, *18*, 799.

[12] T. Mano, T. Kuroda, S. Sanguinetti, T. Ochiai, T. Tateno, J. Kim, T. Noda, M. Kawabe, K. Sakoda, G. Kido, N. Koguchi, *Nano Lett.* **2005**, *5*, 3.

[13] T. Noda, T. Mano, M. Jo, T. Kawazu, H. Sakaki, *J. Appl. Phys.* **2012**, *112*, 063510.

[14] C. Somaschini, S. Bietti, N. Koguchi, F. Montalenti, C. Frigeri, S. Sanguinetti, *Appl. Phys. Lett.* **2010**, *97*, 053101.

[15] J. Skiba–Szymanska, R. M. Stevenson, C. Varnava, M. Felle, J. Huwer, T. Müller, A. J. Bennett, J. P. Lee, I. Farrer, A. B. Krysa, P. Spencer, L. E. Goff, D. A. Ritchie, J. Heffernan, A. J. Shields, *Phys. Rev. Appl.* **2017**, *8*, 014013.

[16] R. S. R. Gajjela, P. M. Koenraad, *Nanomaterials* **2021**, *11*, 85.

[17] M. Anderson, T. Müller, J. Huwer, J. Skiba-Szymanska, A. B. Krysa, R. M. Stevenson, J. Heffernan, D. A. Ritchie, A. J. Shields, *npj Quantum Information 2020* **6**, 14.

[18] E. M. Sala, Y. I. Na, M. Godsland, A. Trapalis, J. Heffernan, *Phys. Status Solidi RRL* **2020**, *14*, 2000173.

[19] M. Anderson, T. Müller, J. Skiba-Szymanska, A. B. Krysa, D. A. Ritchie, A. J. Shields, *Appl. Phys. Lett.* **2021**, *118*, 014003.

[20] J. M. Garcıa, G. Medeiros-Ribeiro, K. Schmidt, T. Ngo, J. L. Feng, A. Lorke, J. Kotthaus, P. M. Petroff, *Appl. Phys. Lett.* **1997**, *71*, 2014.

[21] C. Paranthoen, N. Bertru, O. Dehaese, A. Le Corre, S. Loualiche, B. Lambert, G. Patriarche, *Appl. Phys. Lett.* **2001**, *78*, 1751.

[22] G. Costantini, A. Rastelli, C. Manzano, P. Acosta–Diaz, R. Songmuang, G. Katsaros, O. G. Schmidt, K. Kern, *Phys. Rev. Lett.* **2006**, *96*, 226106.

[23] G. D. Lian, J. Yuan, L. M. Brown, G. H. Kim, D. A. Ritchie, *Appl. Phys. Lett.* **1998**, *73*, 49.

[24] F. Ferdos, S. Wang, Y. Wei, A. Larsson, M. Sadeghi, Q. Zhao, *Appl. Phys. Lett.* **2002**, *81*, 1195.

[25] G. Costantini, A. Rastelli, C. Manzano, R. Songmuang, O. G. Schmidt, K. Kern, H. Von Känel, *Appl. Phys. Lett.* **2004**, *85*, 5673.

[26] J. M. Ulloa, C. Çelebi, P. M. Koenraad, A. Simon, E. Gapihan, A. Letoublon, N. Bertru, I. Drouzas, D. J. Mowbray, M. J. Steer, M. Hopkinson, *J. Appl. Phys.* **2007**, *101*, 081707.

[27] C. Cornet, C. Levallois, P. Caroff, H. Folliot, C. Labbé, J. Even, A. Le Corre, S. Loualiche, M. Hayne, V. V. Moshchalkov, *Appl. Phys. Lett.* **2005**, *87*, 233111.

[28] F. Guffarth, R. Heitz, A. Schliwa, O. Stier, N. N. Ledentsov, A. R. Kovsh, V. M. Ustinov, D. Bimberg, *Phys. Rev. B* **2001**, *64*, 085305.

[29] J. Tatebayashi, M. Nishioka, Y. Arakawa, *Appl. Phys. Lett.* **2001**, *78*, 3469.

[30] P. Klenovský, V. Křápek, D. Munzar, J. Humlíček, *Appl. Phys. Lett.* **2010**, *97*, 203107.

[31] P. Steindl, E. M. Sala, B. Alén, D. Fuertes Marrón, D. Bimberg, P. Klenovský, *Phys. Rev. B* **2019**, *100*, 195407.

[32] G. Stracke, E. M. Sala, S. Selve, T. Niermann, A. Schliwa, A. Strittmatter, D. Bimberg, *Appl. Phys. Lett.* **2014**, *104*, 123107.

[33] M. Jo, T. Mano, K. Sakoda, *J. Appl. Phys.* **2010**, *108*, 083505.

[34] R. Beanland, *Ultramicroscopy* **2005**, *102*, 115.

[35] D. M. Bruls, J. W. A. M. Vugs, P. M. Koenraad, H. W. M. Salemink, J. H. Wolter, *Appl. Phys. Lett.* **2002**, *81*, 1708.

[36] M. Bugajski, W. Lewandowski, *J. Appl. Phys.* **1985**, *57*, 521.

[37] A. Schliwa, M. Winkelnkemper, D. Bimberg, *Phys. Rev. B* **2007**, *76*, 205324.

[38] M. A. Herman, D. Bimberg, J. Christen, *J. Appl. Phys.* **1991**, *70*, 2.

[39] P. Paki, R. Leonelli, L. Isnard, R. A. Masut, *J. Vac. Sci. Technol. A* **2000**, *18*, 3.